

Synthesis and Characterization of Mixed-Metal Aryloxo-Organometallic Precursors for Oxide–Ceramic Materials

Łukasz John,[†] Józef Utka,[†] Sławomir Szafert,[†] Lucjan B. Jerzykiewicz,[†] Leszek Kępiński,[‡] and Piotr Sobota^{*,†}

Faculty of Chemistry, University of Wrocław, 14 F. Joliot-Curie, 50-383 Wrocław, Poland, and Institute of Low Temperature and Structure Research, Polish Academy of Sciences in Wrocław, 2 Okólna, 50-422 Wrocław, Poland

Received August 10, 2007. Revised Manuscript Received April 4, 2008

Potential single-source molecular precursors $[\text{Ba}\{(\mu\text{-ddbfo})_2\text{MR}_x\}_2]$ ($\text{ddbfoH} = 2,3\text{-dihydro-2,2-dimethylbenzofuran-7-ol}$; $\text{M/R/x} = \text{Al/Me/2}$, Al/Et/2 , Ga/Me/2 , or Zn/Et/1) for mixed metal oxide materials were prepared by the reaction of barium aryloxo $[\text{Ba}(\text{ddbfo})_2(\text{ddbfoH})_2] \cdot 3\text{ddbfoH}$ with an appropriate organometallic compound in toluene. The precursors were characterized by elemental analysis, IR and NMR spectroscopy, and single-crystal X-ray structural analysis. The Ba/Al_2 and Ba/Ga_2 complexes undergo thermal decomposition to give mixed metal oxides BaM_2O_4 ($\text{M} = \text{Al}$, at $1300\text{ }^\circ\text{C}$ for both Me and Et derivatives; Ga, at $1430\text{ }^\circ\text{C}$). Instead, the Ba/Zn_2 complex decomposes to a mixture of BaCO_3 and different metal oxides. The chemical composition and surface morphology of heterobimetallic oxides were analyzed by SEM-EDS and X-ray powder diffraction (XRD) that revealed the formation of highly pure oxide materials with micrometer particle sizes.

Introduction

For the last two decades, there has been a growing interest in the development of the chemistry of mixed-metal bi- and polynuclear oxo-, alkoxo- and alkoxo-organometallic complexes. Such interest derives from their fascinating structural chemistry, interesting catalytic properties, and high potential for industrial applications.¹ High applicability of such compounds is an effect of a cooperation of two different metals in a single molecule which gives rise to properties that are not a simple sum of the properties of the individual metals and is often crucial for a system to achieve the desired activity. The classical example would be the cooperation of titanium and aluminum in an olefin polymerization catalyst.² Instead, well-defined group 2 heterobimetallic alkoxo complexes are known as very efficient single-source precursors (SSP) for the fabrication of highly pure oxide–ceramic materials.³ These are crucial for today's technology and are utilized for the production of superconductors, microelectronic circuits, sensors, and ferroelectric materials. Also most computer chips contain oxide components.

The fact that most of the heterobimetallic alkoxo species can generate bimetallic or multimetallic oxides has resulted

in high research activity in the field. The literature cites many ways to prepare high purity metal oxides. For instance, alkoxides or alkoxo-organometallic complexes are perfect candidates for sol–gel and MOCVD (metal–organic chemical vapor-phase deposition) conversion to appropriate oxide products.⁴ Many other techniques like ion implantation, plasma spray, or electrodeposition of ceramic powders may also be used to obtain the desired composites.⁵ “Single-source” bimetallic compounds can generate ceramic materials in a single step. Such materials deliver both elements of a final product eliminating the need to match the reaction rates required from a multicomponent precursor mixture. Extremely important in this technique is the fact that the desired stoichiometry is achieved on the molecular level. This is due to the selective formation of the heterometallic compound, which can be subsequently thermolyzed to yield the targeted highly pure oxide product.⁶

Among many possible heterobimetallic complexes, those which contain alkaline-earth metals have lately attracted some special interest. Magnesium containing compounds are for instance excellent polymerization initiators or substrates for halogen exchange reactions.⁷ Barium containing compounds are a little scarcer although some interesting examples were lately published.⁸

The population of structurally characterized heterobimetallic complexes of heavier alkaline-earth metals is not significantly

[†] University of Wrocław.

[‡] Polish Academy of Sciences in Wrocław.

- (1) Bradley, D. C.; Mehrotra, R. C.; Rothwell, I. P.; Singh, A. *Alkoxo and Aryloxo Derivatives of Metals*; Academic Press: London, 2001.
- (2) (a) Haltky, G. G. *Chem. Rev.* **2000**, *100*, 1347. (b) Chen, E. Y.-X.; Marks, T. J. *Chem. Rev.* **2000**, *100*, 1391.
- (3) (a) Fernandez-Garcia, M.; Martinez-Arias, A.; Hanson, J. C.; Rodriguez, J. A. *Chem. Rev.* **2004**, *104*, 4063. (b) Tian, L.; Lye, W. H.; Deivaraj, T. C.; Vittal, J. J. *Inorg. Chem.* **2006**, *45*, 8258. (c) Labouthee, A.; Wongkasemjit, S.; Traversa, E.; Laine, R. M. *J. Eur. Ceram. Soc.* **2000**, *20*, 91. (d) Mathur, S.; Veith, M.; Ruegamer, T.; Hemmer, E.; Shen, H. *Chem. Mater.* **2004**, *16*, 1304. (e) Mathur, S.; Shen, H.; Veith, M. *J. Am. Ceram. Soc.* **2006**, *89*, 2027.

- (4) (a) Cheng, B.; Shi, W.; Russell-Tanner, J. M.; Zhang, L.; Samulski, E. T. *Inorg. Chem.* **2006**, *45*, 1208. (b) Chandler, C. D.; Roger, C.; Hampden-Smith, M. J. *Chem. Rev.* **1993**, *93*, 1205. (c) Kessler, V. G. *J. Sol-Gel Sci. Technol.* **2004**, *32*, 11. (d) Tahir, A. A.; Molloy, K. C.; Mazhar, M.; Kociok-Köhn, G.; Hamid, M.; Dastgir, S. *Inorg. Chem.* **2005**, *44*, 9207.
- (5) (a) Caulton, K. G. *Chem. Rev.* **1990**, *90*, 969. (b) Segal, D. *J. Mater. Chem.* **1997**, *7* (8), 1297.
- (6) Veith, M. *J. Chem. Soc., Dalton Trans.* **2002**, 2405.

large and includes some alkoxo, alkoxo-hydride, and alkoxo-organometallic complexes.¹ For example, Veith and co-workers recently reported some well-defined barium/group 4 metal complexes [BaZr₂(O^tBu)₁₀],⁹ [BaTi₃(OⁱPr)₁₄],¹⁰ and [Ba₂Zr-(O^tBu)₈(HO^tBu)]·2THF.⁹ Also Hubert-Pfalzgraf and co-workers reported some very interesting barium-copper and barium-yttrium species [YBa₂(HFIP)₇(THF)₃], [BaCu-(HFIP)₄(DME)₂], [Y₂Ba(HFIP)₄(thd)₄], [BaCu₂(HFIP)₄(thd)₂], and [YCu(HFIP)(thd)] (HFIP = 1,1,1,3,3,3-hexafluoro-2-propoxide; thdH = 2,2,6,6-tetramethyl-3,5-heptanedione).¹¹ In our research group we have also synthesized several structurally interesting heterobimetallic alkoxo-organometallic complexes containing second group metals.¹² Lately we have published a few interesting calcium aluminum species containing alkoxo and aryloxo ligands.^{12a} In this paper, we report results of our further study on the subject and present the synthesis of a few mixed-metal aryloxo-organometallic barium complexes, an excellent single-source precursors for oxide materials.

Experimental Data

All reactions were conducted under dinitrogen using standard Schlenk techniques. Solvents were treated as follows: toluene, distilled from Na/benzophenone; hexanes, distilled from P₂O₅. AlMe₃, GaMe₃, ZnEt₂, and ddbfoH (2,3-dihydro-2,2-dimethylbenzofuran-7-ol) were obtained from Aldrich and used without further purification unless stated otherwise. Infrared spectra were recorded on a Perkin-Elmer 180 spectrophotometer in Nujol mulls. Thermogravimetric-differential thermal analyses (TGA-DTA) were recorded on a Setaram SETSYS 16/18. The thermolyzed products were characterized recording X-ray powder diffraction (XRD) patterns with a DRON-1 diffractometer using Cu K α radiation (λ = 1.5418 Å) filtered with Ni. The measurements were done for 2θ = 5–120° with the 2θ step = 0.1°. Microscope analyses were performed with a Philips SEM 515 microscope equipped with an EDAX 9800 spectrometer (30 kV, linear resolution 5 nm). NMR spectra were obtained on a BRUKER ESP 300E spectrometer. GC-MS analyses were recorded on a gas chromatograph with a mass detector HP 5971A and an infrared detector HP5965B (Hewlett-Packard). Microanalyses were conducted with an ARL Model 3410 + ICP spectrometer (Fisons Instruments) and a VarioEL III CHNS (in-house). Thermal decompositions were performed using Tube Furnace PR-50/1800.

[Ba(ddbfO)₂(ddbfOH)₂]·3ddbfOH (1·3ddbfOH). A Schlenk flask fitted with a reflux condenser with a N₂ inlet/oil bubbler was charged with metal Ba (2.43 g; 17.69 mmol), 20.00 mL of 2,3-dihydro-

2,2-dimethyl-7-benzofuranol (ddbfoH; 22.02 g; 132.76 mmol), and 10 mL of C₆H₅CH₃. The mixture was stirred at 90 °C until all the metal was consumed (usually 6–7 h). The mixture was cooled down to room temperature and filtered, and the volatiles were removed by oil pump vacuum. A total of 80 mL of hexanes was added to the resulting oily powder, and the mixture was stirred for 15 min. The white precipitate was filtered off, washed with hexanes (3 × 15 mL), and dried to give **1·3ddbfOH** as a white powder (13.56 g, 10.56 mmol, 60%). Calcd for C₇₀H₈₂O₁₄Ba (1284.70): C, 65.44; H, 6.43. Found: C, 65.29; H, 6.41. Colorless blocks of **1·3ddbfOH** were grown by layering hexanes over a toluene solution of **1·3ddbfOH**.

¹H NMR (CDCl₃, 298 K): δ = 10.8 (br s, OH), 7.42–6.62 (m, 3H of Ph), 2.69 (s, CH₂), 1.38 (s, 2CH₃). ¹³C{¹H} NMR (CDCl₃, 298 K): δ = 147.3 (s, C(O_{phenoxo})C(O)), 144.4 (s, C(O_{phenoxo})), 127.4 (s, C(H)C(CH₂)), 121.9 (s, (CH)CH(CH)), 116.6 (s, (CH)CH(C)), 115.1 (s, C(O_{phenoxo})CH(CH)), 88.1 (s, C(CH₃)₂), 43.7 (s, CH₂), 27.9 (s, 2CH₃).

[Ba(μ -ddbfo)₂AlMe₂]₂ (2-Me). A Schlenk flask was charged with **1·3ddbfOH** (1.85 g; 1.44 mmol) and C₆H₅CH₃ (60 mL). The clear solution was stirred vigorously at 0 °C, and 4.32 mL of AlMe₃ (2 M solution in C₆H₅CH₃; 8.72 mmol) was added dropwise. The reaction was warmed to room temperature. After 0.5 h the solution became cloudy. The suspension was stirred for 24 h, and the white precipitate was filtered off.¹³ The clear solution was reduced in volume to approximately 40 mL. After 72 h colorless block crystals were formed. They were filtered off, washed with hexanes (3 × 10 mL), and dried by oil pump vacuum to give **2** in 76% yield (0.99 g; 1.09 mmol). Calcd for C₄₄H₅₆Al₂BaO₈ (904.19): C, 58.45; H, 6.24. Found: C, 58.22; H, 6.17. IR (cm⁻¹, Nujol mull): 1890 (vw), 1810 (vw), 1616 (vs), 1588 (m), 1490 (vs), 1462 (vs), 1372 (s), 1310 (vs), 1288 (s), 1236 (m), 1192 (s), 1160 (m), 1132 (s), 1112 (s), 1056 (m), 1038 (vs), 968 (w), 902 (w), 866 (s), 844 (m), 768 (vs), 720 (s), 672 (s), 590 (m), 528 (w), 496 (w), 478 (m), 376 (w).

¹H NMR (toluene-*d*₈, 298 K): δ = 7.04–6.58 (m, 3H of Ph), 2.56 (s, CH₂), 1.23 (s, 2CH₃), -0.17 (s, 2Al-CH₃). ¹³C{¹H} NMR (toluene-*d*₈, 298 K): δ = 152.3 (s, C(O_{phenoxo})C(O)), 151.4 (s, C(O_{phenoxo})), 129.1 (s, C(H)C(CH₂)), 127.3 (s, (CH)CH(CH)), 120.3 (s, (CH)CH(C)), 118.1 (s, C(O_{phenoxo})CH(CH)), 93.6 (s, C(CH₃)₂), 46.8 (s, CH₂), 32.1 (s, 2CH₃), -4.8 (s, 2Al-CH₃). GC-MS: analysis confirmed a MeH evolution during reaction. Purity of BaAl₂O₄ (%): C, 0.03; H, 0.00. SEM-EDS: Ba:Al = 0.5 (0.01).

[Ba(μ -ddbfo)₂AlEt₂]₂ (2-Et). **1·3ddbfOH** (0.85 g; 0.66 mmol), C₆H₅CH₃ (40 mL), and 3.30 mL of AlEt₃ (1.0 M solution in C₆H₅CH₃; 3.30 mmol) were combined in a procedure analogous to that for **2-Me**. The analogous workup gave after 96 h colorless block crystals of **2-Et**. They were filtered off, washed with hexanes (3 × 10 mL), and dried by oil pump vacuum to give **2-Et** in 43% yield (0.27 g; 0.28 mmol). Calcd for C₄₈H₆₄Al₂BaO₈: C, 60.03; H, 6.73. Found: C, 58.87; H, 7.04. IR (cm⁻¹, Nujol mull): 1888 (vw), 1814 (vw), 1616 (vs), 1594 (m), 1486 (vs), 1466 (vs), 1375 (s), 1306 (vs), 1285 (s), 1240 (m), 1192 (s), 1158 (m), 1133 (s), 1111 (s), 1056 (m), 1043 (vs), 898 (s), 856 (s), 788 (s), 712 (w), 650 (s), 614 (m), 596 (w), 448 (s), 424 (s), 390 (w).

¹H NMR (toluene-*d*₈, 298 K): δ = 7.05–6.45 (m, 3H of Ph); 2.51 (s, CH₂); 1.24 (s, 2CH₃); 1.67 (t, 2Al-CH₂CH₃); 0.53 (q, 2Al-CH₂CH₃). ¹³C{¹H} NMR (toluene-*d*₈, 298 K): δ = 147.4 (s, C(O_{phenoxo})C(O)), 144.5 (s, C(O_{phenoxo})), 126.6 (s, C(H)C(CH₂)), 123.1 (s, (CH)CH(CH)), 117.8 (s, (CH)CH(C)), 115.5 (s, C(O_{phenoxo})CH(CH)), 90.0 (s, C(CH₃)₂), 43.7 (s, CH₂), 28.3 (s, 2CH₃),

- (7) (a) Hsieh, H. L.; Wang, I. W. *Macromolecules* **1986**, *19*, 299–304. (b) Inoue, A.; Kitagawa, K.; Shinokuba, H.; Oshima, K. *J. Org. Chem.* **2001**, *66*, 4333.
 (8) (a) Zuniga, M. F.; Deacon, G. B.; Ruhlandt-Senge, K. *Chem. Eur. J.* **2007**, *13*, 1921. (b) Westerhausen, M. *Dalton Trans.* **2006**, 4755.
 (9) Veith, M.; Mathur, S.; Huch, V.; Decker, T. *Eur. J. Inorg. Chem.* **1998**, 1327.
 (10) Veith, M.; Mathur, S.; Huch, V. *Inorg. Chem.* **1997**, *36*, 2391.
 (11) Labrize, F.; Hubert-Pfalzgraf, L. G.; Daran, J.-C.; Halut, S.; Tobaly, P. *Polyhedron* **1996**, *15*, 2707.
 (12) (a) Utiko, J.; Ejfler, J.; Szafert, S.; John, L.; Jerzykiewicz, L. B.; Sobota, P. *Inorg. Chem.* **2006**, *45*, 5302. (b) Jerzykiewicz, L. B.; Utiko, J.; Sobota, P. *Organometallics* **2006**, *25*, 4924. (c) Utiko, J.; Lizurek, A.; Jerzykiewicz, L. B.; Sobota, P. *Organometallics* **2004**, *23*, 296. (d) Utiko, J.; Przybylak, S.; Jerzykiewicz, L. B.; Szafert, S.; Sobota, P. *Chem. Eur. J.* **2003**, *9*, 181. (e) Sobota, P. *Coord. Chem. Rev.* **2004**, *248*, 1047. (f) Sobota, P.; Utiko, J.; Sztajnowska, K.; Ejfler, J.; Jerzykiewicz, L. B. *Inorg. Chem.* **2000**, *39*, 235. (g) Utiko, J.; Szafert, S.; Jerzykiewicz, L. B.; Sobota, P. *Inorg. Chem.* **2005**, *44*, 5194.

- (13) This precipitate is most probably the aluminum aryloxo [AlMe₂(ddbfo)]₂. In a similar reaction of **1** with InMe₃ the dimeric [InMe₂(ddbfo)]₂ was isolated in analytically pure form.

19.9 (s, 2Al-CH₂CH₃), 10.9 (s, 2Al-CH₂CH₃). Purity of BaAl₂O₄ (%): C, 0.04; H, 0.00.

[Ba{(μ -ddbfo)₂GaMe₂}] (3). 1·3ddbfoH (1.17 g; 0.91 mmol), C₆H₅CH₃ (40 mL), and 2.30 mL of GaMe₃ (2 M solution in C₆H₅CH₃; 4.55 mmol) were combined in a procedure analogous to that for **2**. The analogous workup gave after 48 h colorless cubic crystals of **3**. They were filtered off, washed with cold hexanes (3 × 10 mL), and dried by oil pump vacuum to give 0.56 g of analytically pure product (62%; 0.57 mmol). Calcd for C₄₄H₅₆O₈BaGa₂ (989.66): C, 53.40; H, 5.70; Ba, 13.87. Found: C, 52.56; H, 6.13; Ba, 14.10. IR (cm⁻¹, Nujol mull): 1884 (vw), 1700 (vw), 1612 (vs), 1580 (m), 1486 (vs), 1308 (vs), 1286 (s), 1234 (m), 1192 (m), 1160 (m), 1130 (s), 1112 (m), 1056 (m), 1034 (s), 968 (vw), 870 (s), 840 (w), 776 (s), 764 (vs), 748 (s), 720 (s), 620 (m), 600 (m), 574 (s), 540 (m), 488 (m), 472 (m), 368 (vw).

¹H NMR (toluene-*d*₈, 298 K): δ = 7.03–6.41 (m, 3H of Ph), 2.56 (s, CH₂), 1.25 (s, 2CH₃), -0.29 (s, 2Ga-CH₃). ¹³C{¹H} NMR (toluene-*d*₈, 298 K): δ = 151.5 (s, (C(O_{phenoxo}))C(O)), 150.4 (s, C(O_{phenoxo})), 129.5 (s, C(H)C(CH₂)), 126.2 (s, (CH)CH(CH)), 119.3 (s, (CH)CH(C)), 117.3 (s, C(O_{phenoxo})CH(CH)), 92.4 (s, C(CH₃)₂), 47.2 (s, CH₂), 31.5 (s, 2CH₃), -1.3 (s, 2Ga-CH₃). GC-MS: analysis confirmed a MeH evolution during the reaction. Purity of BaGa₂O₄ (%): C, 0.04; H, 0.00. SEM-EDS: Ba:Ga = 0.5 (0.01).

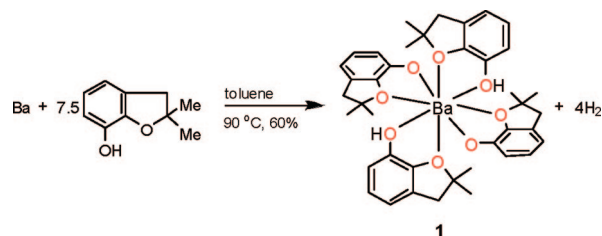
[Ba{(μ -ddbfo)₂ZnEt₂}] (4). 1·3ddbfoH (1.20 g; 0.93 mmol), C₆H₅CH₃ (40 mL), and 5.00 mL of ZnEt₂ (1.0 M solution in hexanes; 5.00 mmol) were combined in a procedure analogous to that for **2**. A similar workup (10 mL of hexanes were added to the filtrate) gave after one week colorless pillar crystals. They were filtered off, washed with cold hexanes (3 × 10 mL), and dried by oil pump vacuum to give **4** in 47% yield (0.43 g; 0.44 mmol). Calcd for C₄₄H₅₄O₈BaZn₂ (978.95): C, 53.98; H, 5.56; Ba, 14.03. Found: C, 54.11; H, 5.37; Ba, 13.56. IR (cm⁻¹, Nujol mull): 1884 (vw), 1704 (vw), 1610 (s), 1578 (m), 1484 (vs), 1458 (s), 1368 (m), 1306 (vs), 1284 (s), 1262 (w), 1232 (m), 1190 (w), 1160 (m), 1136 (m), 1104 (m), 1052 (m), 1036 (s), 956 (vw), 940 (vw), 872 (s), 840 (w), 780 (m), 760 (s), 744 (m), 736 (w), 720 (s), 696 (vw), 616 (m), 574 (m), 518 (w), 484 (w), 462 (w), 368 (vw).

¹H NMR (toluene-*d*₈, 298 K): δ = 7.11–6.46 (m, 3H of Ph), 2.53 (s, CH₂), 1.58 (s, CH₃), 1.37–1.32 (m, 3H of 2Zn-CH₂CH₃), 0.40–0.36 (m, 2H of 2Zn-CH₂CH₃). GC-MS: analysis confirmed a EtH evolution during reaction.

Oxide Preparation. In a typical procedure the precursor was heated at the desired temperature for 5 h. After decomposition, oxide products were identified by XRD. The morphologies and elemental compositions of BaAl₂O₄ and BaGa₂O₄ particles were investigated using scanning electron microscopy–energy-dispersive spectrometry (SEM-EDS). Carbon and hydrogen contaminations were examined by elemental analysis.

Details of X-ray Data Collection and Reduction. Data were collected using a KUMA KM4 CCD (ω scan technique) diffractometer equipped with an Oxford Cryosystem-Cryostream cooler. The space groups were determined from systematic absences and subsequent least-squares refinement. One frame checked every 50 frames showed no crystal decay. Lorentz and polarization corrections were applied. The structures were solved by direct methods and refined by full-matrix-least-squares on F^2 using the SHELXTL Package.¹⁴ Non-hydrogen atoms were refined with anisotropic thermal parameters. Hydrogen atom positions were calculated and

Scheme 1. Synthesis of 1



added to the structure factor calculations but were not refined. Scattering factors, and $\Delta f'$ and $\Delta f''$ values, were taken from the literature.¹⁵

All data (except structure factors) have been deposited with the Cambridge Crystallographic Data Centre in association with earlier communications (**1**·3ddbfoH and **2**-Me)^{12g} or as supplementary publications CCDC 648548 (**2**-Et), CCDC-648549 (**3**), and CCDC-648550 (**4**). Copies of the data can be obtained free of charge by application to CCDC, 12 Union Road, Cambridge CB21EZ, UK (e-mail: deposit@ccdc.cam.ac.uk).

Results and Discussion

Synthesis of 1. As mentioned in the introduction, well-defined heterobimetallic alkoxides are excellent single-source precursors (SSP) for the oxide-ceramic materials. The literature describes few basic routes of their preparation,¹ and of all these methods the ones with homoleptic substrates are especially useful. Hence, as an initial point of our project, we prepared the mononuclear barium 7-benzofuranoxide [Ba(ddbfo)₂(ddbfoH)]₂·3ddbfoH (ddbfoH = 2,3-dihydro-2,2-dimethylbenzofuran-7-ol); **1**·3ddbfoH) that was easily obtained in a direct reaction of metallic barium with an excess of ddbfoH in toluene as shown in Scheme 1. The workup gave **1**·3ddbfoH in 60% isolated yield as colorless crystals. The air-sensitive compound is soluble in aromatic hydrocarbons and CH₂Cl₂ and can be stored under N₂ for extended periods.

Compound **1**·3ddbfoH gave correct microanalysis and was characterized by NMR spectroscopy (¹H and ¹³C) as summarized in Experimental Section. ¹H NMR showed that all ligands are equivalent in solution (one set of proton signals), suggesting their mutual interaction through numerous hydrogen bonds. This is further supported by a very broad singlet of the OH group located at 10.79 ppm.

The TGA analysis of **1**·3ddbfoH shows the melting to start at 128 °C, which followed by slow decomposition that at approximately 160 °C leads to a mass loss of 40.6%. Further heating to >600 °C gives rise to an overall mass loss of 73.5% which corresponds to the extrusion of four ligand moieties. No MS analysis of the volatiles was performed.

Crystal Structure of 1·3ddbfoH. Crystallization of **1**·3ddbfoH from the biphasic toluene/hexanes system gave colorless crystals, and the crystal structure was determined as outlined in the Experimental Section and Table 1.

(14) Sheldrick, G. M. *SHELXTL*, version 5.10; Bruker AXS Inc.: Madison, WI.

(15) Cromer, D. T.; Waber, J. T. In *International Tables for X-ray Crystallography*; Ibers, J. A., Hamilton, W. C., Eds.; Kynoch: Birmingham, U.K., 1974; Vol. 4, pp 72–98, 149–150; Tables 2.2B and 2.3.1.

Table 1. Crystallographic Data for 1·3ddbfoH–4

	complex				
	1·3ddbfoH	2-Me	2-Et	3	4
chemical formula	C ₇₀ H ₈₂ BaO ₁₄	C ₄₄ H ₅₆ BaAl ₂ O ₈	C ₄₈ H ₆₄ BaAl ₂ O ₈	C ₄₄ H ₅₆ BaGa ₂ O ₈	C ₄₄ H ₅₄ BaZn ₂ O ₈
formula weight	1284.70	904.19	960.29	989.66	978.95
temp (K)	100(1)	100(1)	100(1)	85(1)	100(1)
space group	<i>P</i> 2 ₁ / <i>c</i>	<i>C</i> 2/ <i>c</i>	<i>P</i> $\bar{1}$	<i>C</i> 2/ <i>c</i>	<i>P</i> $\bar{1}$
<i>a</i> [Å]	20.147(3)	12.500(2)	12.991(3)	12.474(5)	10.508(5)
<i>b</i> [Å]	14.825(3)	17.710(2)	18.174(4)	17.861(5)	11.444(5)
<i>c</i> [Å]	21.798(3)	20.468(2)	21.696(4)	20.432(5)	19.927(5)
α [deg]	90.0	90.0	67.58(3)	90.0	89.2(1)
β [deg]	99.13(2)	103.25(1)	88.40(3)	103.26(5)	82.2(1)
γ [deg]	90.0	90.0	89.16(3)	90.0	70.3(1)
<i>V</i> [Å ³]	6428.1(18)	4410.5(10)	4733.3(17)	4431(2)	2234(2)
<i>Z</i>	4	4	4	4	2
ρ [g/cm ³]	1.327	1.362	1.348	1.484	1.454
μ (Mo K α) [mm ⁻¹]	0.682	0.989	0.924	2.135	1.984
R1 (>2 σ)	0.0440	0.0378	0.0334	0.0228	0.0365
wR2 (>2 σ)	0.0736	0.0744	0.0777	0.0461	0.0685

Refinement showed mononuclear species with four O,O'-chelating ligands in the metal coordination sphere and three ligand molecules in the outer sphere. The molecular structure of 1·3ddbfoH is shown in Figure 1, and the key metrical parameters are given in Table 2. In the complex molecule the metal atom is surrounded by four bidentate ligands. The eight-coordinating barium atom remains between 2.835(19) and 2.696(2) Å from the oxygen atoms. Such values are much higher than those in [Ba₂(Odpp)(μ -Odpp)₃]¹⁶ (2.488(2) Å; Odpp = 2,6-diphenylphenolate) suggesting the presence of neutral OH groups in the proximity of the barium atom.

Indeed, closer analysis of the O–H and O···H distances showed that in the solid state the neutral ddbfoH molecules remain in the coordination sphere of barium. From this perspective, 1·3ddbfoH should formally be regarded as an ionic compound [Ba(ddbfoH)₄][ddbfo]₂·ddbfoH with two anionic ddbfo ligands and one neutral benzofuranol outside the coordination sphere of the metallic cation. Similar compounds with organic¹⁷ and metal containing anions outside the coordination sphere were reported.¹⁸

Synthesis of 2–4. The presence of neutral 7-benzofuranols in the barium coordination sphere made 1·3ddbfoH an attractive target for the transformation into a heterobimetallic species via O metalation. A similar proton abstraction approach to heterobimetallic compounds has

lately been explored by Singh and Roesky.¹⁹ In their work a large variety of heterobimetallic oxo complexes were obtained from metal hydroxides and appropriate organometallic precursors. A similar approach has also been utilized by Mehrotra and co-workers for the synthesis of group 2 metal aluminates.²⁰

As shown in Scheme 2 the organometallics AlMe₃, AlEt₃, GaMe₃, or ZnEt₂ were combined with 1·3ddbfoH in toluene at 0 °C. Workups gave heterobimetallic [Ba{(μ -ddbfo)₂AlMe₂}] (Ba^{Me}Al₂; 2-Me), [Ba{(μ -ddbfo)₂AlEt₂}] (Ba^{Et}Al₂; 2-Et), [Ba{(μ -ddbfo)₂GaMe₂}] (Ba/Ga₂; 3), and [Ba{(μ -ddbfo)₂ZnEt₂}] (Ba/Zn₂; 4) as colorless crystalline species in 43–76% yields. They were unstable in the air but could be stored under dinitrogen for weeks. They are soluble in most organic solvents excluding aliphatic hydrocarbons. Compounds 2–4 were characterized by elemental analysis and IR and NMR (¹H and ¹³C) spectroscopy as summarized in Experimental Section.

In all the reactions there is an organometallic driven abstraction of the OH protons from the barium inner sphere 7-benzofuranols. This leads to the subsequent evolution of methane (2-Me and 3) or ethane (2-Et and 4) and results in a linkage of benzofuranoxo ligands to form a pair of four-coordinating ligands in which the buckling role is played by the MR_x⁺ (2-Me and 3, R = Me, *x* = 2; 2-Et, R = Et, *x*

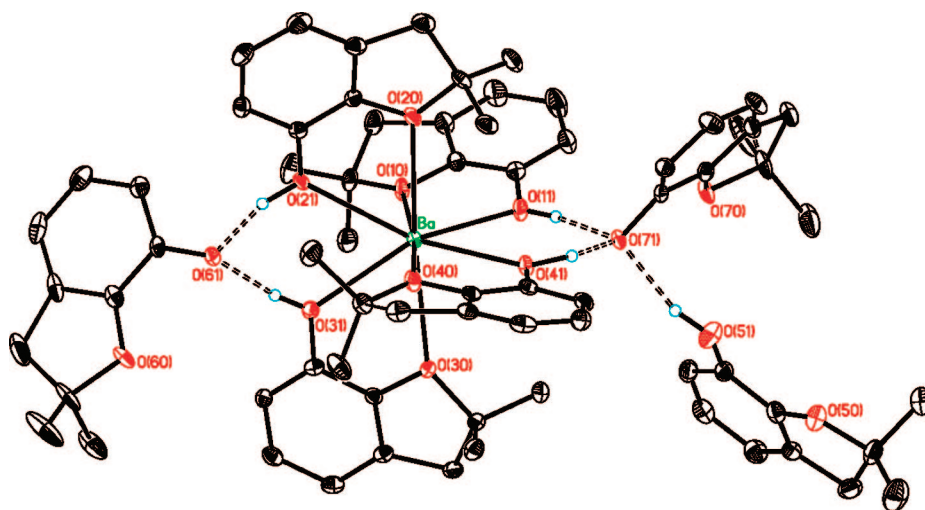


Figure 1. View of 1·3ddbfoH.

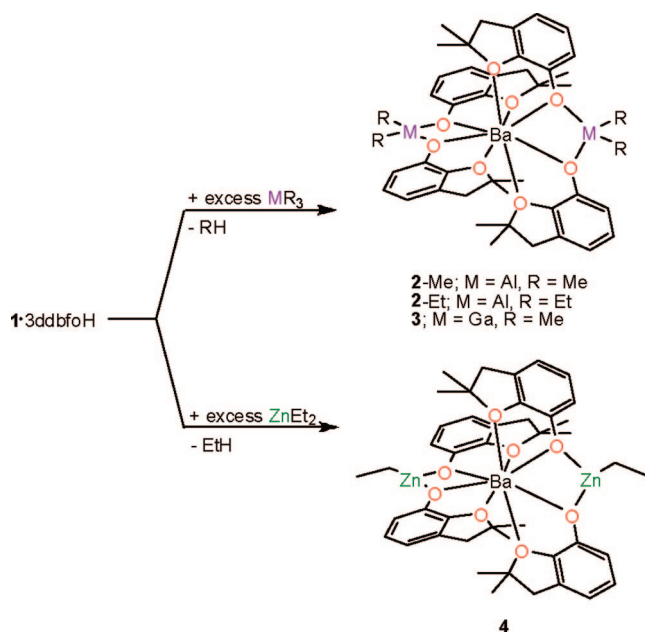
Table 2. Selected Bond Lengths (Å) and Angles (deg) for 1·3ddbfoH–4

	1·3ddbfoH	2-Me	2-Et	3	4	
Ba1–O(10)	2.835(19)	2.8189(18)	2.7839(19)	2.8086(19)	2.788(2)	2.825(2)
Ba1–O(11)	2.762(2)	2.7281(17)	2.7457(18)	2.7742(17)	2.7570(15)	2.791(2)
Ba1–O(20)	2.835(19)	2.787(2)	2.801(2)	2.820(2)	2.8290(19)	2.859(2)
Ba1–O(21)	2.728(19)	2.7795(18)	2.770(2)	2.750(2)	2.7121(16)	2.739(2)
Ba1–O(30)	2.832(18)		2.8194(18)	2.7918(18)		2.794(2)
Ba1–O(31)	2.696(2)		2.7493(18)	2.7543(18)		2.764(2)
Ba1–O(40)	2.778(18)		2.8434(19)	2.8063(19)		2.898(3)
Ba1–O(41)	2.714(18)		2.7738(18)	2.7773(18)		2.748(2)
M'1–O(11)		1.8081(19)	1.8119(19)	1.8051(19)	1.9167(15)	1.953(2)
M'1–O(21)		1.811(2)	1.8094(19)	1.8070(19)	1.9165(13)	1.9519(19)
M'2–O(31)			1.8076(18)	1.8158(19)		1.947(2)
M'2–O(41)			1.8106(19)	1.813(2)		1.956(2)
M'1–C(1)		1.962(3)	1.976(3)	1.973(3)	1.964(2)	1.961(3)
M'1–C(2)		1.964(4)	1.985(3)	1.980(3)	1.966(2)	
M'2–C(3)			1.973(3)	1.975(3)		1.966(3)
M'2–C(4)			1.978(3)	1.975(3)		
Ba–O(11)–M'1		109.65(8)	108.40(8)	107.62(8)	109.67(7)	106.92(13)
Ba–O(21)–M'1		107.49(8)	107.52(8)	108.52(9)	111.47(7)	108.93(13)
Ba–O(31)–M'2			108.69(9)	108.13(9)		108.41(12)
Ba–O(41)–M'2			107.61(9)	107.31(9)		108.68(12)

= 2; 4, R = Et, $x = 1$) moieties as shown in Scheme 2. The proposed structures of 2–4 are nicely supported by ^1H NMR spectra. In 2 and 3 a signal pattern of aromatic protons similar to that found in the free ligand is observed. Also well-developed signals corresponding to organometallic fragments are observed at -0.17 for 2-Me, 1.67 (t, CH_3), and 0.53 (q, CH_2) for 2-Et and at -0.29 ppm for 3. Moreover, in ^{13}C NMR the carbon atoms of the alkyl group of MR_2^+ fragment are observed at -4.8 for 2-Me, 19.9 (s, CH_2) and 10.9 (s, CH_3) for 2-Et, and -1.3 ppm for 3.

The ^1H NMR of 4 showed the right resonances of ethyl CH_2 and CH_3 groups at 0.40 – 0.36 and 1.37 – 1.32 ppm, respectively, but the pattern of aromatic protons of the ddbfo ligand was not so straightforward as for 2 and 3. Here the region was much more complex, exhibiting a set of multiplets located between 7.11 and 6.46 ppm. This along with the lowest solubility of 4 within a series suggested additional interactions that were further confirmed by X-ray analysis. Because of the low solubility of 4, the ^{13}C NMR spectrum has not been measured.

Scheme 2. Syntheses of 2–4



Crystal Structures of 2–4. The crystal structures of 2–4 were determined as outlined in Table 1 and described in the Experimental Section.

Figure 2 (top and center) presents molecules of complexes 2 and 3 that are isomorphic. The bottom view shows a superposition of both complexes. They crystallize in monoclinic space group $C2/c$ as colorless block crystals.

Both neutral complexes are composed of one barium atom and two group 3 atoms. The barium atom is surrounded by eight oxygen atoms of four ddbfo ligands. Each aluminum/gallium atom is four-coordinate and is occupied by two donor oxygen atoms of aryloxo ligands and two carbon atoms of methyl groups. The Ba–O bond distances (see Table 2) range from $2.728(17)$ to $2.819(17)$ Å in 2-Me and from $2.712(16)$ to $2.829(19)$ Å in 3, which is comparable to other Ba–O bond distances reported in the literature for mixed-metal compounds.^{8–11,16,21,22} The Al–O bond distances in 2 fall within $1.808(18)$ and $1.811(19)$ Å, and the Al–C distances are $1.962(3)$ and $1.964(3)$ Å.

Barium and aluminum/gallium centers are bridged by aryloxo oxygen atoms of benzofuranoxide ligands. The bridging Ba–O–M' bond angles equal $109.65(8)$ and $107.49(8)^\circ$ for 2-Me and $109.67(7)$ and $111.47(7)$ for 3.

The compound 2-Et crystallizes in the $P\bar{1}$ space group with two molecules in the asymmetric unit. The molecule of 2-Et is “isostructural” to those of 2-Me and 3 and is presented in Figure 3.

The coordination mode of both Ba and Al atoms is identical and the metric parameters are very close to those of 2-Me.

Also the molecular structure of 4 is similar to those of 2 and 3. The complex crystallizes in the triclinic system and shows an eight-coordinate barium atom bound to four deprotonated benzofuranoxo ligands. The two ZnEt^+ moieties are coordinated to aryloxo oxygen atoms. The zinc centers are three-coordinate. Such a coordination number on a zinc site has already been observed in $\text{Ba}[\text{Zn}(\text{CH}_2\text{SiMe}_3)_3]_2$, $(\text{THF})_4\text{Ca}[(\text{MeZn})_2(\mu\text{-PSi}^i\text{Pr}_3)_2]$, and $[(\text{THF})\text{BaN}(\text{SiMe}_3)_2]_2\text{-Zn}_4\text{Et}_2(\text{PSi}^i\text{Bu}_3)_4$.^{8b}

Ba–O distances in 4 (Figure 4) are within the $2.739(2)$ – $2.791(2)$ Å range for Ba–O_(alkoxo) and $2.794(2)$ – $2.898(3)$ Å

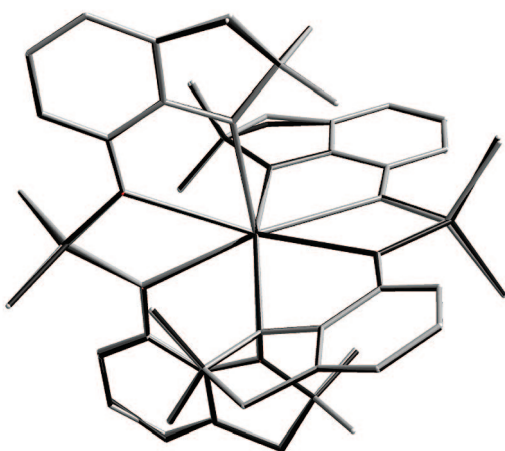
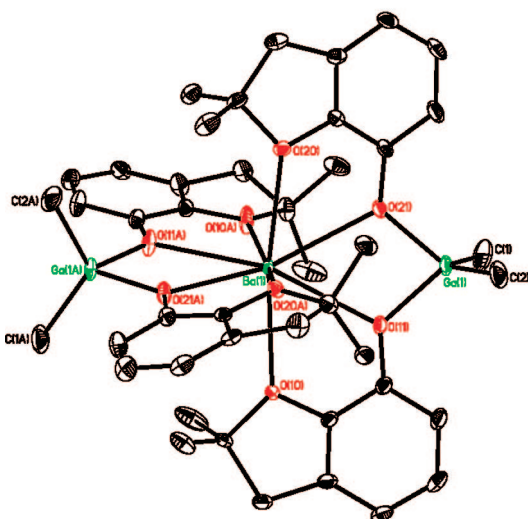
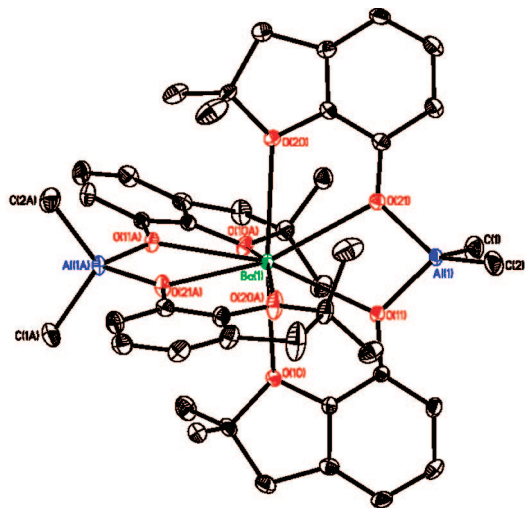


Figure 2. Molecular structure of 2-Me (top), 3 (center), and their superposition (bottom; light grey, 2-Me; dark grey, 3).

for Ba–O_(ether) distances. The O_(alkoxo)–Ba–O_(alkoxo) bond angles range from 55.99(5) to 144.17(5)°. The Zn(1)–O(11), Zn(1)–O(21), Zn(2)–O(31), and Zn(2)–O(41) distances are 1.954(18), 1.952(18), 1.947(19), and 1.956(19) Å, respectively. The O(11)–Zn(1)–O(21) and O(31)–Zn(2)–O(41) bond angles are 83.34(8) and 83.50(7)°, respectively. More-

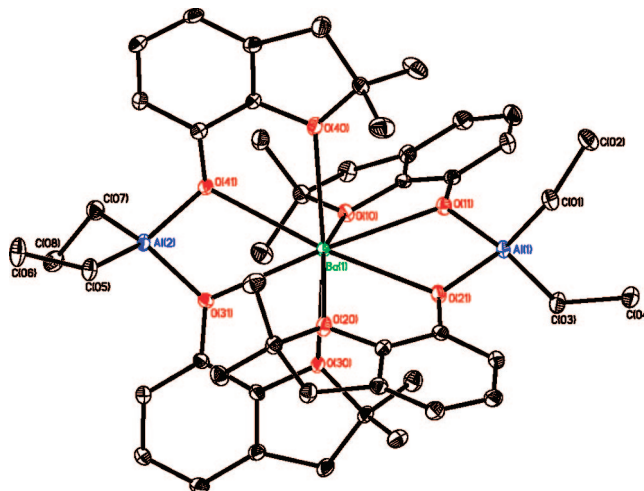


Figure 3. Molecular structure of 2-Et.

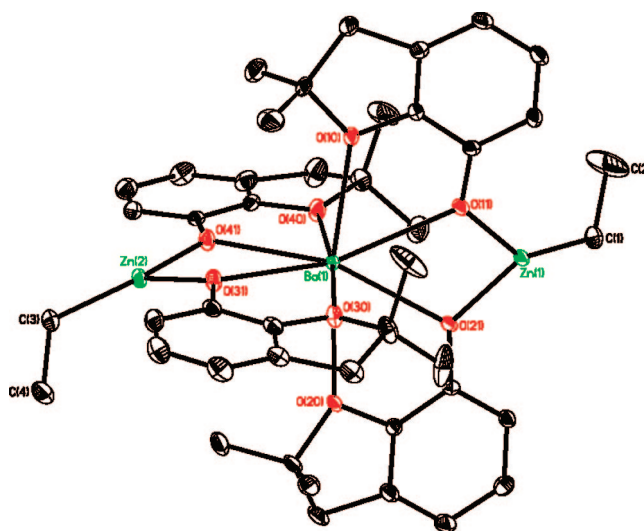


Figure 4. Molecular structure of 4.

over, bond angles between O(11)–Zn(1)–C(1), O(21)–Zn(1)–C(1), O(31)–Zn(2)–C(3), and O(41)–Zn(2)–C(3) are 136.76(10), 133.83(10), 137.83(10), and 135.79(10)°, respectively. All bond distances and angles are comparable to those reported in the literature.^{21a,22a,23} Although the

- (16) Deacon, G. B.; Forsyth, C. M.; Junk, P. C. *J. Organomet. Chem.* **2000**, 607, 112.
- (17) Love, C. P.; Torardi, C. C.; Page, C. *J. Inorg. Chem.* **1992**, 31, 1784.
- (18) (a) Kanters, J. A.; Smeets, W. J. J.; Venkatasubramanian, K.; Poonia, N. S. *Acta Crystallogr., Sect. C* **1984**, 40, 1701. (b) Day, V. W.; Eberspacher, T. A.; Frey, M. H.; Klemperer, W. G.; Liang, S.; Payne, D. A. *Chem. Mater.* **1996**, 8, 330.
- (19) Singh, S.; Roesky, H. W. *Dalton Trans.* **2007**, 1360.
- (20) Sharma, M.; Singh, A.; Mehrotra, R. C. *Synth. React. Inorg. Met.-Org. Chem.* **2002**, 32, 1223.
- (21) (a) Arion, V. B.; Bill, E.; Reetz, M. T.; Goddard, R.; Stöckigt, D.; Massau, M.; Levitsky, V. *Inorg. Chim. Acta* **1998**, 282, 61. (b) Petrella, A. J.; Craig, D. C.; Lamb, R. N.; Raston, C. L.; Roberts, N. K. *Dalton Trans.* **2004**, 327. (c) Evans, W. J.; Giarikos, D. G.; Greci, M. A.; Ziller, J. W. *Eur. J. Inorg. Chem.* **2002**, 453. (d) Petrella, A. J.; Roberts, N. K.; Craig, D. C.; Raston, C. L.; Lamb, R. N. *Chem. Commun.* **2003**, 2288.
- (22) (a) van Veggel, F. C. J. M.; Harkema, S.; Bos, M.; Verboom, W.; Woolthuis, G. K.; Reinhoudt, D. N. *J. Org. Chem.* **1989**, 54, 2351. (b) Guillemot, G.; Solari, E.; Rizzoli, C.; Floriani, C. *Chem.-Eur. J.* **2002**, 8, 2072. (c) van Veggel, F. C. J. M.; Bos, M.; Harkema, S.; Verboom, W.; Reinhoudt, D. N. *Angew. Chem., Int. Ed.* **1989**, 28, 746.

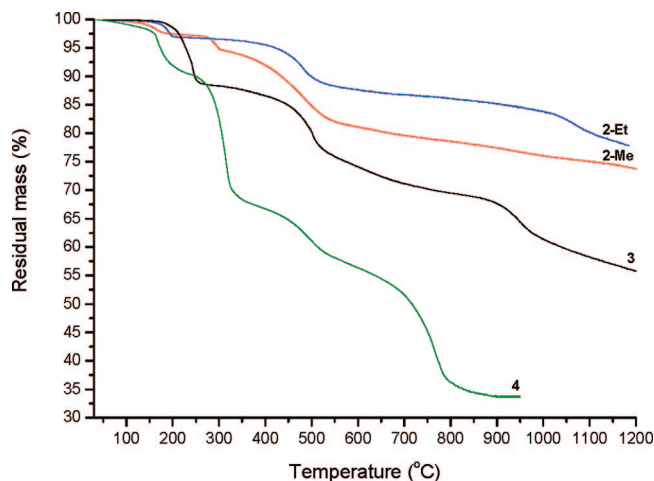


Figure 5. TGA curves of 2–4.

coordination number of the zinc atom seems to be three, the earlier mentioned obscurities in a signal pattern of the phenyl ring in the ^1H NMR spectrum of **4**, compared to **2** and **3**, suggested the possible existence of the long distance agostic $\text{Zn}\cdots\text{C}$ interaction. Careful analysis indeed showed the contact of the zinc atom with a carbon atom of the neighboring phenyl ring of 2.897 Å. Similar contacts were observed in $[\text{Zn}(\text{2-methylallyl})_2]$ (2.919(1) Å).²⁴

Thermogravimetry and Powder XRD of 2–4. Hetero-bimetallic 2–4 were next tested as sources for oxide materials. They all have the correct ratio of metals to serve as precursors for double oxides. The thermal decomposition of 2–4 was investigated first with the use of TGA analysis under N_2 , and the results are presented in Figure 5. It clearly shows that 2–4 when heated from room temperature up to 1200 °C within 4 h underwent multistep noncompleted thermal decomposition. The curves show that the inception of decomposition (weight loss) occurs at 128, 180, 188, and 185 °C for 2-Me, 2-Et, 3, and 4, respectively. TGA as well as microscopic observations showed no signs of sublimation.

Within the temperature range 25–1200 °C the precursor 2-Me undergoes three major stages of weight loss. The first one occurring at 128–210 °C is associated with a 2.7% loss of the initial mass. The second occurs at 210–350 °C and is characterized by a 3.6% loss of the initial mass. Finally, the third noticeable weight loss (13.9% of the initial mass) is observed at 350–680 °C, and further slow decomposition takes place up to and over 1200 °C. As to the higher homologue 2-Et, the first mass loss (3.2%) occurs at 180–220 °C. The other two appear at 483–580 °C and 1010–1200 °C (9.0 and 10.0% of initial mass loss, respectively) showing that the exchange of the R group at the aluminum center slightly increased decomposition temperatures. Precursor 3 also decomposes in three observable steps in the temperature regions 188–410 °C (13.7%), 410–840 °C (17.3%), and 840–1025 °C (8.5% of the initial mass loss). Finally, compound 4 (at the temperature range 25–950 °C) decomposes in four steps in temperature regions of 185–270

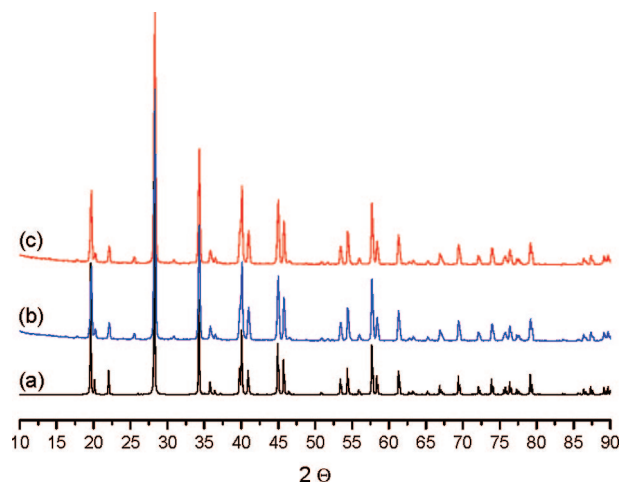


Figure 6. XRD patterns: (a) BaAl_2O_4 (ICSD 10036), (b) precursor 2-Me, and (c) 2-Et (both decomposed at 1300 °C).

°C (11.3% mass loss), 270–420 °C (22.6% weight loss), 420–625 °C (10.7% of initial weight loss), and between 625 and 830 °C with 20.5% loss of the initial mass. Unfortunately, the subsequent weight losses observed in TGA experiments (similarly as for $1\cdot 3\text{ddbfoH}$) do not correspond with the weight losses that could be predicted when a specific number of ligands was liberated. From this perspective no clean processes were observed for $1\cdot 3\text{ddbfoH}$ –4. Moreover, as can be clearly noticed at the TGA curves for 2-Me, 2-Et, and 3, further mass loss can be predicted for all compounds above 1200 °C which in our opinion is related to thermal stability of barium carbonate (probable intermediate) at this temperature. Also the fact that all the experiments were carried out in anaerobic conditions might be the cause of not definite thermal decomposition of 2–4 that is evident due to the light gray color of the residues suggesting substantial content of organic material. In general, decomposition of metal aryloxides is much more challenging compared to that alkoxo derivatives. Metal complexes with chelating and bulky aryloxo groups are nonvolatile and much more stable than monodentate alkoxides. Hence, thermal decomposition of metal aryloxo derivatives is much more complex and usually a long lasting process.

On the basis of phase diagrams compounds 2–4 were next thermolyzed in oxidative atmosphere (air). The resulting materials were analyzed by XRD analysis. The diffraction patterns shown in Figure 6 that were obtained for 2-Me and 2-Et thermolyzed at 1300 °C are identical with that for BaAl_2O_4 reported in the literature.²⁵ The diffraction peaks obtained for precursor 3 thermolyzed at 1430 °C match exactly those of BaGa_2O_4 as shown in Figure 7.²⁶ For all these precursors no residual peaks of BaCO_3 were observed at lower 2θ values ($2\theta < 10^\circ$). The XRD pattern for compound 4 which was thermolyzed at above 1000 °C can be assigned to the mixture of BaCO_3 and ZnO reported in

(23) Uhlenbrock, S.; Wegner, R.; Krebs, B. *J. Chem. Soc., Dalton Trans.* **1996**, 3731.

(24) Benn, R.; Grondy, H.; Lehmkuhl, H.; Nehl, H.; Angermund, K.; Krüger, C. *Angew. Chem., Int. Ed. Engl.* **1987**, *26*, 1279.

(25) (a) Hoerkner, W.; Mueller-Buschbaum, H. *Z. Anorg. Allg. Chem.* **1979**, *451*, 40. (b) Tomaszewski, P. *Phase Transitions* **1992**, *38*, 127.

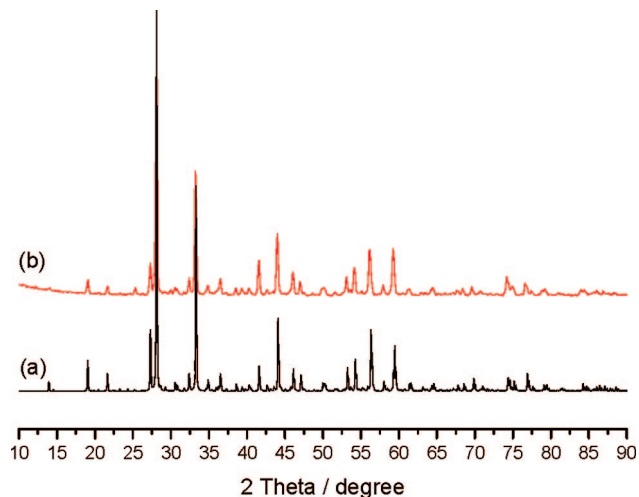


Figure 7. XRD patterns: (a) β -BaGa₂O₄ (ICSD 91281) and (b) precursor **3** decomposed at 1430 °C.

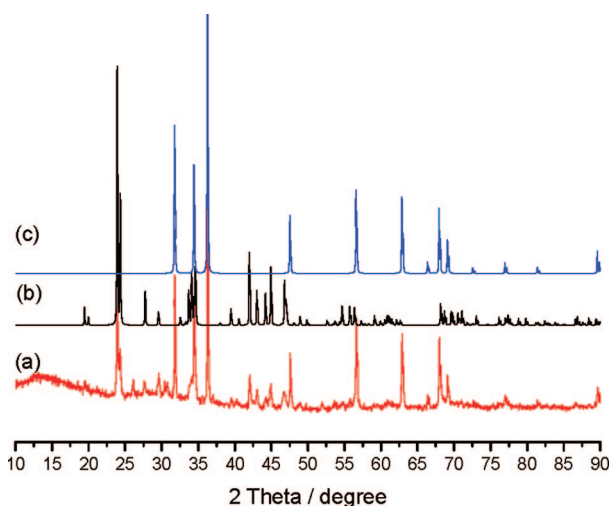


Figure 8. XRD patterns: (a) precursors **4** decomposed at 1000 °C, (b) BaCO₃ (ICSD 15196), and (c) ZnO (ICSD 26170).

the Inorganic Crystal Structure Database (see Figure 8).²⁷ Later, when the BaCO₃–ZnO system was thermolyzed at the temperatures up to and above 1200 °C, further decomposition was observed to finally give a mixture of BaCO₃, BaO, ZnO, and mixed metal oxides BaZnO₂ and Ba₂ZnO₃. Elemental analysis of the final powder did not match any specific mixture of oxides.²⁸

SEM-EDS Analysis. The morphology and elemental composition of the **2-Me** and **3** samples were determined by SEM and EDS analyses (see Figures 9 and 10). Standardless EDS analyses performed on many grains revealed a Ba:M atomic ratio of 0.50 ± 0.01 for **2-Me** and **3**. No other elements except oxygen were detected in the EDS spectra (residual carbon content from the high purity conducting carbon tabs used to fix the powder samples was identified). The presence of carbonate residues was excluded by additional analysis (elemental analysis, Fourier transform

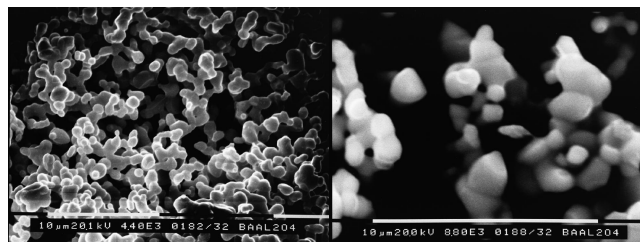


Figure 9. SEM micrographs of BaAl₂O₄.

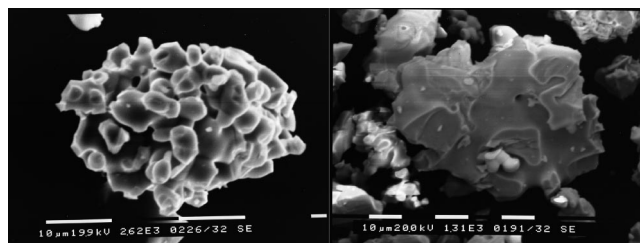


Figure 10. SEM micrographs of BaGa₂O₄.

infrared, and XRD analysis in the lower 2θ values). Results of EDS analyses are consistent with the phase identification by XRD, where BaAl₂O₄ (precursor **2-Me**) and BaGa₂O₄ (precursor **3**) appear to be the only compounds present in the samples.

Conclusions

In conclusion, we have presented a simple, high-yield synthetic route to access barium-containing heterobimetallic species, potential single-source precursors for oxide-ceramic materials. This synthetic method comprises reaction of barium aryloxide with appropriate organometallic agents. The presented method is an alternative to conventional methods and the Pechini process²⁹ and comprises SSP-I/SSP-II precursors.⁶

Monobarium aluminate²⁵ and monobarium gallate^{26,30} were first prepared by conventional methods. The major disadvantages of these methods are that the final oxide product is not pure and, in many cases, the metal to metal ratio is not strictly determined. We have demonstrated that the compounds **2** and **3** exemplify effective precursors for heterobimetallic oxides of composition BaM₂O₄, where M = Al and Ga. As showed by SEM-EDS analysis that double oxide samples are highly pure. Spinel of composition AB₂O₄ (where A = Ca²⁺, Sr²⁺, Ba²⁺; B = Al³⁺, Ga³⁺) are known to show interesting ferroic properties. Moreover, such double oxides present many different polymorphic forms.^{25,26,30–36} As we have shown, not all of the potential heterobimetallic

(26) (a) Kahlenberg, V.; Fischer, R. X.; Parise, J. B. *J. Solid State Chem.* **2000**, *154*, 612. (b) Kahlenberg, V.; Weidenthaler, C. *Solid State Sci.* **2002**, *4*, 963.

(27) Inorganic Crystal Structure Database, Version 2006-01.

(28) Spitsbergen, U. *Acta Crystallogr.* **1960**, *13*, 197.

(29) Pechini, M. P. U.S. Patent 3,330,697, 1967.

(30) Hoppe, R.; Schepers, B. *Naturwissenschaften* **1960**, *47*, 376.

(31) Suketoshi, I.; Banno, S.; Suzuki, K.; Inagaki, M. *Z. Phys. Chem.* **1977**, *105*, 173.

(32) Suketoshi, I.; Banno, S.; Suzuki, K.; Inagaki, M. *Z. Phys. Chem.* **1977**, *107*, 53.

(33) Huang, S. Y.; von der Mühl, R.; Ravez, J.; Couzi, M. *Ferroelectrics* **1994**, *159*, 127.

(34) Deiseroth, H. J.; Müller-Buschbaum, H. *Z. Anorg. Allg. Chem.* **1973**, *402*, 201.

(35) Schulze, A. R.; Müller-Buschbaum, H. *Z. Anorg. Allg. Chem.* **1981**, *475*, 205.

(36) Müller-Buschbaum, H.; Schmachtel, W. *Z. Naturforsch.* **1976**, *31*, 1605.

precursors can be utilized to form desired double oxide systems. We have presented that compound **4** decomposed at 1000 °C to the mixture of BaCO₃ and ZnO. In a higher temperature (>1200 °C) system, it further decomposes to a mixture of BaCO₃ and mono- and mixed-metal oxides. Even so, compound **4** exemplifies a structurally interesting alkoxo-organometallic compound with three-coordinate zinc atoms. In the literature, there are few known examples of such a rare coordination number on zinc centers.³⁷

(37) (a) Lewiński, J.; Ochal, Z.; Bojarski, E.; Tratkiewicz, E.; Justyniak, I.; Lipkowski, J. *Angew. Chem., Int. Ed.* **2003**, *42*, 4643. (b) Bukhaltsev, E.; Goldberg, I.; Vigalok, A. *Organometallics* **2004**, *23*, 4540.

Acknowledgment. The authors would like to express their gratitude to Prof. Eugeniusz Zych and Mr. Adam Walasek from the Faculty of Chemistry of Wrocław University for their cooperation on powder XRD analysis and to Prof. Tadeusz Lis and Dr. Katarzyna Ślepokura for their expertise in the X-ray analysis of **2-Et**. We thank the Polish State Committee for Scientific Research (Grants N204 101 31/2326 and PBZ-KBN-118/T09/19) for support of this research.

Supporting Information Available: Data for the crystal structures in CIF format and NMR results, TGA data, XRD patterns, and pictures of final oxides after thermal decomposition (PDF). This material is available free of charge via the Internet at <http://pubs.acs.org>.

CM702262N